Positron transport in water vapour

2012 New J. Phys. 14 035003

(http://iopscience.iop.org/1367-2630/14/3/035003)

New Journal of Physics
The open-access journal for physics

Positron transport in water vapour

A Banković[1,6], S Dujko[1], R D White[2], J P Marler[3], S J Buckman[4], S Marjanović[1], G Malović[1], G García[5] and Z Lj Petrović[1]

[1] Institute of Physics, University of Belgrade, PO Box 68, Pregrevica 118, Zemun, Serbia
[2] ARC Centre for Antimatter–Matter Studies, School of Engineering and Physical Sciences, James Cook University, Townsville 4810, QLD, Australia
[3] Northwestern University Evanston, IL 60208, USA
[4] ARC Centre for Antimatter–Matter Studies, The Australian National University, Canberra 0200, ACT, Australia
[5] Instituto de Física Fundamental, Consejo Superior de Investigaciones Científicas, 28006 Madrid, Spain
E-mail: ana.bankovic@gmail.com

New Journal of Physics **14** (2012) 035003 (23pp)
Received 30 November 2011
Published 2 March 2012
Online at http://www.njp.org/
doi:10.1088/1367-2630/14/3/035003

Abstract. Transport properties of positron swarms in water vapour under the influence of electric and magnetic fields are investigated using a Monte Carlo simulation technique and a multi-term theory for solving the Boltzmann equation. Special attention is paid to the correct treatment of the non-conservative nature of positronium (Ps) formation and its explicit and implicit influences on various positron transport properties. Many interesting and atypical phenomena induced by these influences are identified and discussed. Calculated transport properties for positrons are compared with those for electrons, and the most important differences are highlighted. The significant impact of a magnetic field on non-conservative positron transport in a crossed field configuration is also investigated. In general, the mean energy and diffusion coefficients are lowered, while for the measurable drift velocity an unexpected phenomenon arises: for certain values of the reduced electric field, the magnetic field enhances the drift. The variation of transport coefficients with the reduced electric and magnetic fields is addressed using physical arguments with the goal of understanding the synergistic effects of Ps formation and magnetic field on the drift and diffusion of positrons in neutral gases.

[6] Author to whom any correspondence should be addressed.

Contents

1. Introduction

Today positron physics is a large and fruitful area of investigation, interesting not only from the fundamental point of view [1], but also because of many applications that positrons have in different areas, ranging from astrophysics [2] and material science [3] to medicine [4]. The modelling of positron-based technologies or real experimental situations requires knowledge of two types of fundamental data. The first type is collisional data, i.e. the cross-sections for every possible channel of interaction between the positron and the atom/molecule of matter. In the last few decades, a revolutionary breakthrough in atomic physics was made by Surko *et al* [5, 6] who have developed the Penning–Malmerg buffer gas trap for positrons, which now can give high-intensity and high-resolution positron beams for measuring positron cross-sections at low and well-defined energies [7–10]. The second type relying on the cross-section data, is data associated with the transport of positrons in neutral gases and soft-condensed matter [11]. Transport properties are a source of information about a group or ensemble of charged particles travelling through the medium, such as their mean energy, drift velocity and diffusion. Unfortunately, there are limited experimental data on transport coefficients for positrons [12] and only a few groups in the world are directly involved in the modelling of positron transport. A review of the history and current status of positron swarm experiments has been given by Charlton [12] and Petrović *et al* [13].

One of the most important applications of positrons is in medicine, particularly in positron emission tomography (PET) [4]. PET is a technique for diagnostics of the general metabolic activity of the human body and is a key technique for the early detection of cancer. It involves the introduction of a positron-emitting radio-isotope into the body, e.g. ^{18}F, attached to glucose to form a radiopharmaceutical (e.g. fluorodeoxyglucose (FDG)), which targets metabolic activity. This diagnostic technique is assumed to be non-invasive and therefore is widely used in clinical practice. The details of the atomic and molecular processes that take place in human tissue, between the emission of high-energy positrons from the radiopharmaceutical and the detection of the gamma rays, are at present not well quantified.

Many Monte Carlo codes have been specifically developed to model this diagnostic technique [14–18]. Water is the main constituent of living tissue and hence the human body

is usually modelled as a phantom of appropriate geometry filled with liquid water. In order to model the tracks of particles in water [19] one needs to know the cross-sections for interactions of positrons with water, while a knowledge of the secondary electrons, photons and appropriate ions is also important in understanding radiation damage. In spite of the fact that major advances have been made in measuring and collecting the cross-sections for positrons, the current commercial codes either do not deal with positrons at all or at best use only approximate cross-sections for a very few of the processes. In general, in most such codes the interaction of secondary electrons with the tissue is neglected. The authors of those codes seem to have based their approach on the limited experimental data that existed before trap-based beams were applied, e.g. using the cross-sections for electrons to approximate those for positrons, or lumping various cross-sections together, inappropriately. The energy deposition is usually approximated using empirical data, and not based on fundamental positron cross-section data, while the interaction of particles with liquid water is generally presented using the results for interaction with the gas phase scaled to higher density [20].

Another issue associated with the Monte Carlo codes used in PET modelling is the fact that these codes have not been the subject of detailed systematic testing. Validation of theories and associated codes is an important step before their direct application to a more complex situation where many parallel processes occurring on different time and space scales are operative. The procedure we adopt here, which has been applied in low-temperature plasma process modelling, is to benchmark the calculations in the limit of a swarm of charged particles. Benchmark calculations of averaged transport properties for electron swarms under the hydrodynamic and non-hydrodynamic conditions are well established [21–24]. The same strategy should also be applied for Monte Carlo codes used in PET modelling and the errors associated with traditional treatments of positron collision dynamics on various transport properties, including the tracks of positrons, should be identified, highlighted and quantified. One motivation for this paper is to propose a strategy and benchmark for direct comparisons of the various positron simulation and modelling techniques, while highlighting the data required for such a comparison.

Recently, we undertook a programme to compile, evaluate, recommend and disseminate collision and transport data for positrons in neutral gases and soft-condensed matter relevant to various scientific and technological areas [25–32]. One of the main goals was to establish the best and most accurate cross-sections for positron and electron scattering in biologically relevant molecules. Furthermore, it was important to evaluate the transport properties of these particles in neutral gases and soft-condensed matter with the goal of understanding how differences in microscopic antimatter–matter and matter–matter interactions are reflected in the macroscopic transport properties.

For the bio-medical applications of positrons considered here, collision and transport data for positrons in water vapour are required. So, as a first step for this programme, we made a reasonably complete set of cross-sections for positron interactions with water vapour. This cross-section set is complete in the sense that it covers all important processes and therefore provides a good particle, momentum and energy balance. Among the many interesting points associated with this set of cross-sections, perhaps the most important is a large cross-section for Ps formation [10] whose magnitude is comparable to the cross-section for elastic collisions. The compilation and justification of the cross-sections for positrons in water vapour used in this work will be addressed fully in a forthcoming paper. Some of the pertinent data have been reported in an earlier publication [10].

In this paper, we investigate the transport properties for positrons in water vapour. A Monte Carlo simulation code has been applied and our new set of cross-sections for positron scattering in water vapour is used as the input. Since there are no experimental data for positron transport in water vapour, a multi-term theory for solving the Boltzmann equation has been used to validate the results obtained by a Monte Carlo simulation technique. Transport properties for positrons and electrons in water vapour under the influence of the reduced electric field are compared to each other and the most distinct features of their behaviour are discussed. Special attention has been paid to atypical manifestations of the drift and diffusion of positrons caused by the explicit influence of Ps formation. In parallel, the influence of dissociative attachment and ionization on the drift and diffusion of electrons in water vapour has been addressed with the principal idea of identifying the commonality in the basic phenomenology between the positrons and electrons, when the transport is strongly affected by non-conservative collisions. In the second part of this paper, the synergistic effects of magnetic fields and Ps formation on positron transport in crossed electric and magnetic fields are studied. We have been motivated to perform our calculations in a crossed field configuration as possible future applications may use combined fields to achieve better control of positron transport in neutral gases [26] just as was the case for electrons in magnetized plasmas. Values and general trends in the profiles of mean energy, collision frequency, drift velocity elements and diffusion tensor for positrons in water vapour are reported here.

2. Theory: formalism, techniques and methods for the calculation of transport coefficients

Transport coefficients for positrons and electrons presented in this paper are calculated using two entirely different and independent techniques—a Monte Carlo simulation [26, 27] and a multi-term theory for solving the Boltzmann equation [21]. Computer codes behind these methods were originally developed for studying the electron transport in varying configurations of electric and magnetic fields, and they have been the subject of extensive benchmark tests with excellent agreement [21, 22]. Among the many important aspects, special attention has been paid to the correct treatment of non-conservative collisions on various transport properties, which is particularly important for studies of positron transport. For example, the collision operator for Ps formation has the same mathematical form as the attachment operator for electrons within the multi term framework for solving the Boltzmann equation. On the other hand, we found that numerical schemes developed for a correct treatment of the electron attachment within our Monte Carlo simulation technique are fast and accurate for Ps formation. Since Ps formation is a non-conservative process with, generally, a huge cross-section and strong energy dependence, we expect to see its dramatic influence on the profiles of positron transport properties.

2.1. Basic definitions of transport coefficients

In the physics of swarms, the connection between experiment and theory is made through the equation of continuity [33]

$$\frac{\partial n}{\partial t} + \nabla \cdot \mathbf{\Gamma}(\mathbf{r}, t) = S(\mathbf{r}, t), \tag{1}$$

where $n(\mathbf{r}, t)$ is the number density of swarm particles, $\mathbf{\Gamma}(\mathbf{r}, t) = n\langle v\rangle$ is the swarm particle flux and $S(\mathbf{r}, t)$ represents the production rate per unit volume per unit time arising from non-conservative collisional processes. For positrons, these non-conservative processes include Ps formation and annihilation, while for electrons in water vapour we consider the dissociative electron attachment and electron impact ionization. Note that for a positron swarm, the ionization process is a conservative process, i.e. the number of positrons is not affected when this process is operative. In addition, direct annihilation of positrons is not considered here as its magnitude is generally a few orders of magnitude less than the cross-sections for other relevant processes.

Far from boundaries, sources and sinks, the hydrodynamic regime is assumed to apply [34]. In this regime, the space–time dependence of the phase-space distribution function and other transport quantities can be expressed in terms of linear functionals of $n(\mathbf{r}, t)$. A sufficient functional relationship between the phase-space distribution function and number density of swarm particles in the case of weak gradients is the well-known expansion, the so-called hydrodynamic approximation:

$$f(\mathbf{r}, \mathbf{c}, t) = \sum_{s=0}^{\infty} f^{(s)}(\mathbf{c}, t) \odot (-\nabla)^s n(\mathbf{r}, t), \tag{2}$$

where $f^{(s)}(\mathbf{c}, t)$ are time-dependent tensors of rank s and $\odot$ denotes an s-scalar product. Assuming this functional relationship, the flux $\mathbf{\Gamma}(\mathbf{r}, t)$ and source term $S(\mathbf{r}, t)$ in the continuity equation are expanded as

$$\mathbf{\Gamma}(\mathbf{r}, t) = \mathbf{W}_F(t) n(\mathbf{r}, t) - \mathbf{D}_F(t) \cdot \nabla n(\mathbf{r}, t), \tag{3}$$

$$S(\mathbf{r}, t) = S^{(0)} n(\mathbf{r}, t) - \mathbf{S}^{(1)} \cdot \nabla n(\mathbf{r}, t) + \mathbf{S}^{(2)} : \nabla\nabla n(\mathbf{r}, t), \tag{4}$$

where $\mathbf{W}_F$ and $\mathbf{D}_F$ define, respectively, the flux drift velocity and flux diffusion tensor. Substitution of the expansion of the expressions for the source and flux into the continuity equation yields the diffusion equation

$$\frac{\partial n}{\partial t} + \mathbf{W}_B \cdot \nabla n - \mathbf{D}_B : \nabla\nabla n = -R_a n, \tag{5}$$

where

$$R_a = S^{(0)} (\text{loss rate}), \tag{6}$$

$$\mathbf{W}_B = \mathbf{W}_F + \mathbf{S}^{(1)} \text{ (bulk drift velocity)}, \tag{7}$$

$$\mathbf{D}_B = \mathbf{D}_F + \mathbf{S}^{(2)} \text{ (bulk diffusion tensor)}. \tag{8}$$

From the above definitions, it is clear that the difference between the flux and bulk transport coefficients exists only in the presence of non-conservative collisions. This is even more evident if we use the language of a Monte Carlo simulation. In a Monte Carlo simulation, the bulk drift velocity

$$\mathbf{W}_B = \frac{\mathrm{d}}{\mathrm{d}t}\langle \mathbf{r} \rangle \tag{9}$$

and the bulk diffusion tensor

$$\mathbf{D}_B = \frac{1}{2!}\frac{\mathrm{d}}{\mathrm{d}t}\langle \mathbf{r}^\star \mathbf{r}^\star \rangle \tag{10}$$

are determined from the mean position of the electron/positron swarm in configuration space. Here $\mathbf{r}^\star = \mathbf{r} - \langle \mathbf{r} \rangle$, where $\langle \mathbf{r} \rangle$ is the mean position of the swarm. In the absence of non-conservative collisions, one may avoid the differentiation required to calculate the drift velocity and diffusion tensor by using the flux transport coefficients. For example, the flux drift velocity components and the flux diagonal elements of the diffusion tensor can be directly sampled in a Monte Carlo simulation in the following way:

$$W_{F,i} = \left\langle \frac{\mathrm{d}r_i}{\mathrm{d}t} \right\rangle = \langle v_i \rangle, \tag{11}$$

$$D_{F,ii} = \langle r_i v_i \rangle - \langle r_i \rangle \langle v_i \rangle, \tag{12}$$

where v_i is the electron/positron velocity and $i = x, y, z$. It follows from equation (9) that the bulk drift velocity is the displacement of the mean position of the swarm and reflects the motion of the centre of mass of the total ensemble of particles. On the other hand, the flux drift velocity is the mean velocity of particles. One should be aware of the differences in the definition of both sets and make sure that proper data are employed in the models [35].

2.2. A brief overview of the Monte Carlo simulation technique

The Monte Carlo code applied in this work follows a large number of particles ($\sim 10^6$) moving in an infinite gas under the influence of spatially homogeneous electric and magnetic fields [27]. Particles (positrons or electrons) gain energy from the electric field and dissipate this energy through binary collisions with background neutral particles. The charged particle interactions are neglected since the transport is considered in the limit of low charged-particle density. All calculations are performed at zero gas temperature.

In general, at the heart of the Monte Carlo method lies the equation for the collision probability [36]

$$p(t) = \nu_\mathrm{T}(\epsilon(t)) \exp\left(- \int_{t_0}^{t} \nu_\mathrm{T}(\epsilon(t')\mathrm{d}t') \right). \tag{13}$$

This equation gives the probability that the electron/positron will have a collision in the time interval $(t, t + \mathrm{d}t)$, where ν_T is the time-dependent total collision frequency and t_0 is either the time of the electron entering the gas or the time of a previous collision. This equation is solved by numerical integration in small time steps where the time steps are determined by the minimum of two relevant time constants, the mean collision time and cyclotron period for $\mathbf{E} \times \mathbf{B}$ fields. The nature of the collision has been determined using the relative probabilities for individual collisional processes. In this work, all electron/positron scattering is assumed to be isotropic. Transport coefficients are determined after relaxation to steady state using formulae (8)–(12) outlined in the previous subsection and from those given in our previous publications [36–38]. Most importantly, sampling of various dynamic swarm properties has always been performed at times fully uncorrelated with the instants of collisions.

2.3. A brief sketch of the Boltzmann equation analysis

In addition to the Monte Carlo simulation, an alternative approach to the problem of electron/positron transport in neutral gases is through a Boltzmann equation analysis. A swarm

of charged particles moving in an infinite neutral gas under the influence of external electric and magnetic fields is governed by Boltzmann's equation

$$\frac{\partial f}{\partial t} + \mathbf{c} \cdot \frac{\partial f}{\partial \mathbf{r}} + \frac{q}{m} [\mathbf{E} + \mathbf{c} \times \mathbf{B}] \cdot \frac{\partial f}{\partial \mathbf{c}} = -J(f, f_0) \tag{14}$$

for the phase-space distribution function $f(\mathbf{r}, \mathbf{c}, t)$. Here $\mathbf{r}$ and $\mathbf{c}$ represent the position and velocity coordinates, respectively, while q and m are the charge and mass of the swarm particle and t is the time. In this work, we assume that the electric and magnetic fields are spatially homogeneous and stationary. The right-hand side of the Boltzmann equation is the linear charged particle–neutral molecule collision operator, which describes elastic, inelastic and non-conservative collisions. Elastic processes are described using the original Boltzmann collision operator [39], while its semiclassical generalization [40] is applied for inelastic processes. Non-conservative processes are accounted for through the operators detailed in [41, 42].

The methods and techniques for solving the Boltzmann equation are by now standard; for details see recent reviews [21, 33, 43, 44]. Among many important aspects, we emphasize the following important steps in solving Boltzmann's equation:

- No assumptions are made concerning symmetries in velocity space and the directional dependence of the phase-space distribution function in velocity space is represented in terms of spherical harmonic expansion. In contrast to classical two-term theory, no restrictions are placed on the number of spherical harmonics and our method is a truly multi-term approach.
- Assuming the hydrodynamic regime, the spatial (and implicit time) dependence is represented by the hydrodynamic approximation given by equation (2).
- The speed (energy) dependence of the phase-space distribution function is represented by an expansion about a Maxwellian at an arbitrary temperature in terms of Sonine polynomials [41].

Using the appropriate orthogonality relations for the spherical harmonics and modified Sonine polynomials, the Boltzmann equation is converted into a hierarchy of coupled equations for the moments of the distribution function. These equations are numerically solved and all the transport properties are expressed in terms of the moments of the distribution function [21, 33, 44].

3. Results and discussion

3.1. Electron and positron transport properties in water vapour

In this section, transport properties of positrons and electrons in water vapour are calculated as a function of the reduced electric field, E/n_0 (n_0 is the water vapour density) and compared to each other. We consider the electric field range: 1–770 Td (1 Td $= 10^{-21}$ V m^2). The cross-sections for electron scattering in water vapour developed by Hayashi [45] are implemented in this work. Results obtained by a Monte Carlo technique are given by symbols (flux values: full symbols; bulk values: open symbols), while those obtained by a Boltzmann analysis are presented with lines (flux values: solid lines; bulk values: dashed lines).

In figure 1, we show the variation of the mean energy with E/n_0 for electrons and positrons. The mean energy profiles reflect the energy dependence of cross-sections and, in general, one

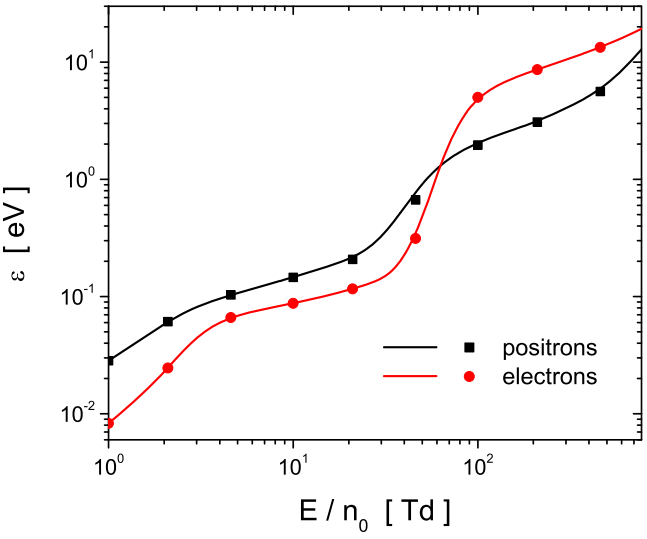

Figure 1. Comparison between the positron and electron mean energies as a function of E/n_0. The results obtained by a Monte Carlo technique are given by symbols, while those obtained by a Boltzmann analysis are presented with lines.

would expect that the mean positron energy dominates the mean electron energy for a fixed E/n_0 (and even for a broad range of E/n_0) due to the smaller number of available inelastic channels. From figure 1, we see that this is true but only for E/n_0 less than 60 Td. Above 60 Td, Ps formation acts in such a manner as to cool the energy distribution function by selectively removing higher-energy positrons. This leads to a lower mean energy for positrons in the E/n_0 range where Ps formation is an increasing function of energy and dominates the inelastic processes.

Figure 2 shows the profiles of the flux and bulk components of the drift velocity for positrons and electrons in water vapour. There is a huge difference between the flux and bulk components of the positron drift velocity. The flux component is a monotonically increasing function of E/n_0, while the most prominent feature in the profile of the bulk drift velocity is the existence of negative differential conductivity (NDC), i.e. over a range of E/n_0 values the drift velocity decreases when the field is increased. NDC is a kinetic phenomenon which has been systematically investigated and explained for electron swarms over the last three decades [46–49]. For positrons, it originates from the non-conservative nature of Ps formation and conditions leading to this phenomenon have been discussed in our previous publications [26–29]. In brief, if the rate of Ps formation is an increasing function of positron energy, positrons are preferentially removed in regions of higher energy, resulting in a shift in the centre-of-mass position, as well as a modification of the spread about the centre of mass. For positrons in water vapour, and in the energy region studied here, the positrons are predominantly removed from the leading edge of the swarm and hence the magnitude of the flux component is greater than the equivalent bulk component. In contrast to electrons, NDC for positrons is present only in the bulk drift velocity component. Comparing NDC for positrons in different gases, this phenomenon is much more pronounced for argon [26, 27] than it is here for water vapour and for H_2 [28, 29]. For N_2, however, the competition between inelastic (electronic excitation) collisions and those which lead to Ps formation removes NDC from the profile of

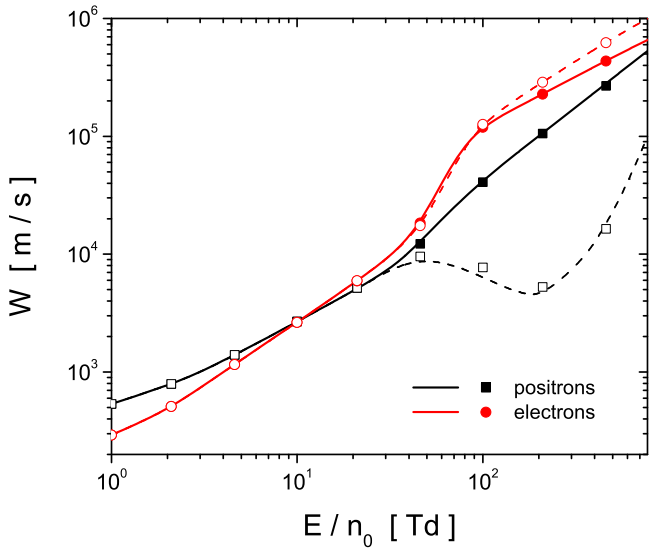

Figure 2. Comparison between the flux and bulk components of the drift velocity for positrons and electrons as a function of E/n_0. The results obtained by a Monte Carlo technique are given by symbols (flux values: full symbols; bulk values: open symbols), whereas those obtained by a Boltzmann analysis are presented with lines (flux values: solid lines; bulk values: dashed lines).

the bulk drift velocity even though the cross-section for Ps formation is high as it is for those gases with very pronounced NDC [30].

Comparing the drift velocity components for electrons and positrons, we observe differences in both shape and magnitude. For the sake of completeness, let us consider the influence of dissociative attachment and electron impact ionization on the drift of electrons. For electrons, the flux and bulk drift velocities start to diverge around 50 Td, where the electron swarm mean energy is approximately 0.5 eV. This difference is very small but noticeable, and favours an enhancement of the flux component. Around 0.5 eV, dissociative attachment begins to play a more significant role. The attachment collision frequency increases with energy, and so the more energetic electrons at the front of the swarm are preferentially attached (see figure 3). This is reflected by the decrease of the bulk drift velocity, i.e. the centre of mass of the swarm is shifted in the direction opposite to the driving electric field. A similar but not identical situation has been previously observed for positrons. The cross-section for Ps formation is many orders of magnitude larger than the corresponding cross-section for dissociative attachment and more importantly the cross-section for Ps formation is much greater than other cross-sections for inelastic collisions. In some cases [27] it is even greater than the cross-section for elastic collisions. This means that the positrons are much more affected by Ps formation than the electrons by dissociative attachment. Returning to electrons, we see that around 90 Td (and a mean energy of approximately 4 eV) there is a crossing over point where the bulk and flux components start diverging again. However, now the opposite situation holds and the bulk is greater than the flux. In this energy range, the rate coefficient for dissociative attachment peaks, the slower electrons are preferentially attached. At the same time the ionization begins to influence the high-energy tail of the distribution function (see figure 3). As a consequence of these two combined non-conservative effects, the centre of the mass is shifted forward in the drift direction.

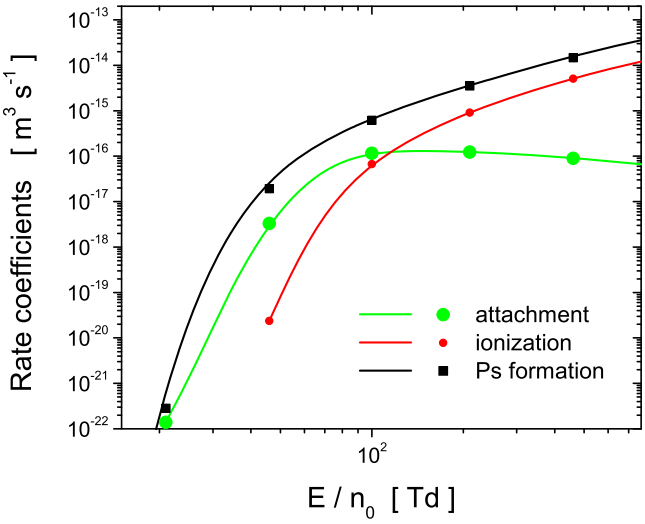

Figure 3. Variations of the rate coefficient for Ps formation for positrons and rate coefficients for dissociative attachment and ionization for electrons with E/n_0. The results obtained by a Monte Carlo technique are given by symbols, while those obtained by a Boltzmann analysis are presented with lines.

Figure 3 displays a comparison of the rate coefficient for Ps formation and rate coefficients for non-conservative processes associated with the electron transport, dissociative attachment and ionization. The rate coefficient for Ps formation dominates over the rate coefficients for the electron impact ionization and dissociative attachment for the E/n_0 range considered in this work. Since there is competition between the electron attachment (which removes electrons from the swarm) and ionization (which increases their number), it is clear that non-conservative effects are less pronounced in electron transport.

The variation of the diffusion coefficients for positron and electron swarms with E/n_0 is displayed in figure 4, where panels (a) and (b) compare the longitudinal and transverse diffusion coefficients, respectively. At low values of E/n_0, diffusion coefficients for positrons are almost an order of magnitude higher than those for electrons. When E/n_0 is increased, the difference further decreases and between 30 and 40 Td the opposite situation holds: diffusion coefficients for electrons become larger than those for positrons. It is clear from figure 4 that the diffusion of positrons is more affected by Ps formation than the diffusion of electrons by the combined effects of dissociative attachment and ionization. A huge difference of almost three orders of magnitude between the flux and bulk components of the longitudinal diffusion coefficient for positrons is observed. Such a difference has never been observed for electron swarms [37, 38, 44, 50].

In figures 5(a) and (b), we highlight the anisotropy of the diffusion tensor and show the comparison between the longitudinal and transverse diffusion coefficients for electron and positron swarms, respectively, in water vapour. We see that the anisotropy of the bulk diffusion tensor for positrons is considerable, with almost two orders of magnitude difference between the bulk components of the longitudinal and transverse diffusion coefficients. The degree of anisotropy for the flux diffusion tensor is not as high. For electrons, the situation is less dramatic. In general, the anisotropy of the flux diffusion tensor follows from a spatial variation of average electron/positron energies within the swarm and energy dependence of

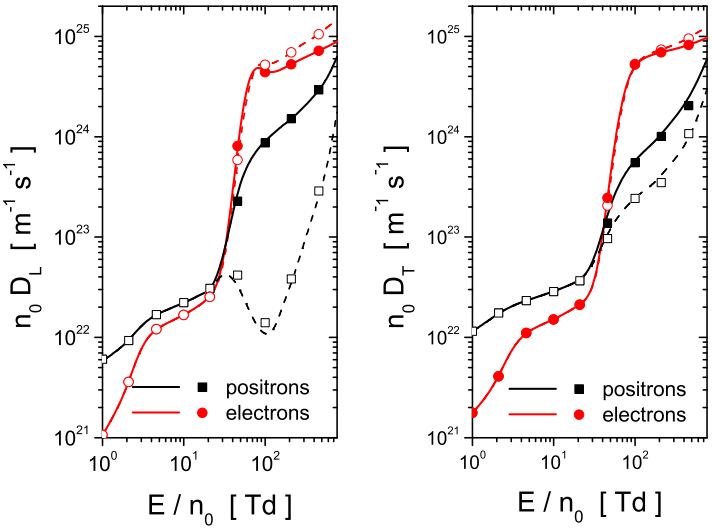

Figure 4. Comparison between the flux and bulk components of the longitudinal (a) and transverse (b) diffusion coefficients for positrons and electrons in water vapour as a function of E/n_0. The results obtained by a Monte Carlo technique are given by symbols (flux values: full symbols; bulk values: open symbols), while those obtained by a Boltzmann analysis are presented with lines (flux values: solid lines; bulk values: dashed lines).

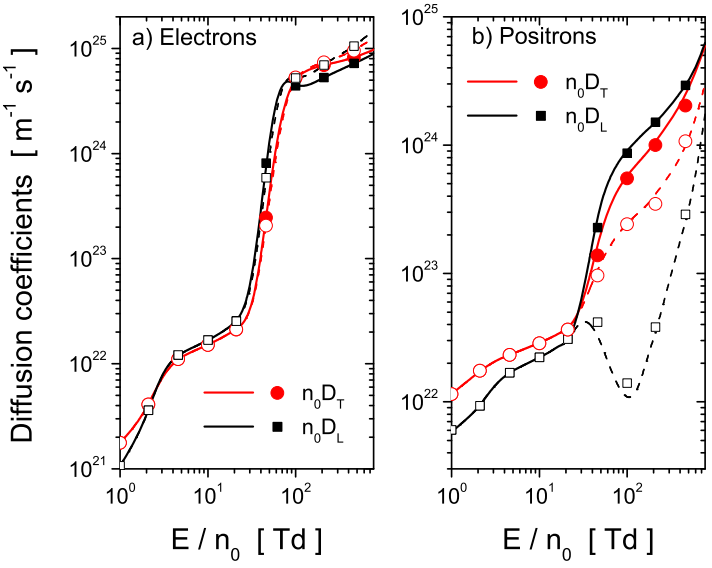

Figure 5. Variation of the diffusion coefficients with E/n_0 for electrons (a) and positrons (b) in water vapour. The results obtained by a Monte Carlo technique are given by symbols (flux values: full symbols; bulk values: open symbols), while those obtained by a Boltzmann analysis are presented with lines (flux values: solid lines; bulk values: dashed lines).

the electron/positron collision frequency. If the electron/positron collision frequency is an increasing function of the energy and if the average energy increases along the swarm, then the particles at the front of the swarm have a higher probability of collision with background

molecules than those at the trailing edge. As a consequence, these two combined effects act to inhibit the diffusion of the swarm longitudinally. This is the well-known diffusion anisotropy effect [44, 51, 52]. Conversely, along the transverse direction, there is no such asymmetry in the local average energy and the anisotropy effect is absent. This is verified in recent Monte Carlo simulations where spatial uniformity in the average energy along the transverse direction is observed [29]. When the electron/positron collision frequency is a decreasing function of energy, the longitudinal diffusion coefficient is higher than the transverse. In such a case, the anisotropy effect enhances the longitudinal diffusion. Of course, the general tendency due to thermal motion for electrons/positrons to disperse in all directions is always present, but this is the only contributing factor in the transverse direction. Similar but not identical behaviour of the diffusion coefficients has been observed for positron swarms in H_2 [29]. For N_2 [30], however, the difference between the flux and bulk diffusion components is drastically reduced by the large inelastic processes (preferentially the electronic excitations) in the vicinity of Ps formation.

From figure 2 we observe that the difference between the drift velocities for positrons and electrons can become higher than two orders of magnitude. The same applies for the diffusion coefficients as observed from figures 4 and 5. This highlights how important it is to employ accurate cross-sections for positron scattering in applications involving positrons. Approximations based on using cross-sections for electron scattering to describe positron behaviour can seriously plague the modelling, and the results may not be even qualitatively correct.

3.2. *Positron transport in water vapour in* $\mathbf{E} \times \mathbf{B}$ *fields*

The application of a magnetic field gives rise to additional transport coefficients as compared to the magnetic field free case. In a crossed field configuration, there are some symmetries among the individual elements of the vector and tensorial transport coefficients. The drift velocity has two independent components, the longitudinal component $W_{\mathbf{E}}$ which describes the drift along the electric field direction and the transverse component $W_{\mathbf{E}\times\mathbf{B}}$ which describes the drift along the $\mathbf{E} \times \mathbf{B}$ direction. The diffusion tensor has three independent diagonal elements, $n_0 D_{\mathbf{E}}$, $n_0 D_{\mathbf{E}\times\mathbf{B}}$ and $n_0 D_{\mathbf{B}}$ in the $\mathbf{E}$, $\mathbf{E} \times \mathbf{B}$ and $\mathbf{B}$ directions, respectively. There are also two individual off-diagonal elements that are not the same and experimentally cannot be individually measured and detected, although together they form the so-called Hall diffusion coefficient which is experimentally detectable. In this section, we investigate the effects of a perpendicular magnetic field on non-conservative positron transport in water vapour. The values of the reduced magnetic field B/n_0 considered in this work are 1000, 2000 and 5000 Hx ($1\,\text{Hx} = 10^{-27}\,\text{T}\,\text{m}^3$).

It is a well-established practice to express the basic phenomenology of charged particle transport in $\mathbf{E} \times \mathbf{B}$ fields in terms of the ratio of the cyclotron to the collision frequency [23, 37, 38, 53]. This ratio for positrons in water vapour is shown as a function of E/n_0 for a range of magnetic field strengths in figure 6. In general, there are three important E/n_0 regions to consider. The first region is the so-called collision dominated regime where the cyclotron frequency is much smaller than the collision frequency ($\Omega \ll \nu_c$). In this region positrons on average may complete only a part of their circular orbit between two collisions. The second important region is the magnetic field controlled regime, where the collision frequency is much smaller than the cyclotron frequency ($\nu_c \ll \Omega$). In this region, positrons, on average, may complete many circular orbits before two succeeding collisions. Between these two regions

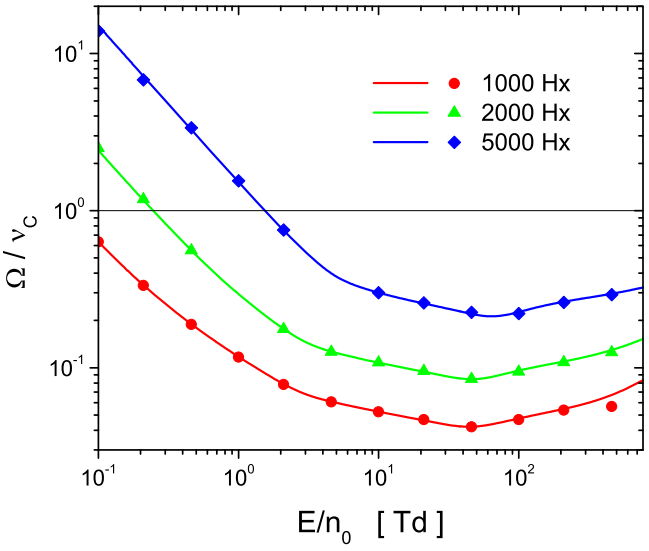

Figure 6. Variation of the ratio between the cyclotron frequency and the collision frequency with E/n_0 for various B/n_0 as indicated on the graph.

there is an intermediate region where the cyclotron and the collision frequency are of the same order ($\Omega \approx \nu_c$). From figure 6 it is evident that an unusually strong magnetic field (much stronger than those required for positrons in N_2 and H_2 [54]) is required to enter the region where the magnetic field controls the behaviour of the swarm. Even for a B/n_0 of 2000 Hx the transport is much more affected by collisions than by the magnetic field, and only for E/n_0 less than 0.3 Td is the dominant role of magnetic field definite. For a magnetic field strength of 5000 Hx, we see that the magnetic field predominantly controls the swarm only for E/n_0 less than 2 Td. In the profiles of the transport coefficients shown below, the distinction between the various regimes is evident.

Figure 7 displays the variation of the mean energy with E/n_0 for a range of B/n_0. The general tendency observed in figure 7 is that the magnetic field cools down the positrons. This follows from the fact that the positrons change the direction of motion due to the magnetic field and hence the electric field cannot efficiently pump energy into the system. This effect is a well-known phenomenon which has been observed many times for electron swarms in atomic and molecular gases [21, 23, 24, 37, 38, 53], and is seen to carry over to positrons. Interestingly, this effect is less pronounced for positrons in water vapour than for positrons in Ar [26], N_2 and H_2 [54]. Due to the complex energy dependence of the collision frequency, in conjunction with the cooling mechanisms induced by Ps formation, one can identify the regions of E/n_0 where the mean energy is almost insensitive to the presence of a magnetic field. This unusual physical situation has not been observed for electrons in gases where the mean energy is a monotonically decreasing function of the applied magnetic field.

3.2.1. Drift and NDC for positrons in $\mathbf{E} \times \mathbf{B}$ *fields.* The drift of the positron swarm can be described in terms of a drift speed at some angle to the direction of electric field (magnetic deflection angle). Figure 8 displays the flux and bulk components of the drift speed as a function of E/n_0, while the magnetic deflection angle ϕ is presented in figure 9. We see that there is now no NDC effect in the drift speed profiles for non-zero magnetic fields. In other words, when a

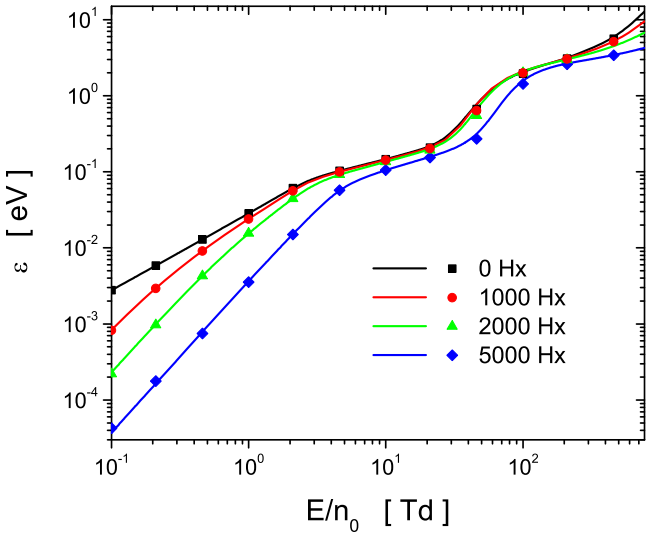

Figure 7. Variation of the mean energy for positron swarm with E/n_0 for various B/n_0 as indicated on the graph.

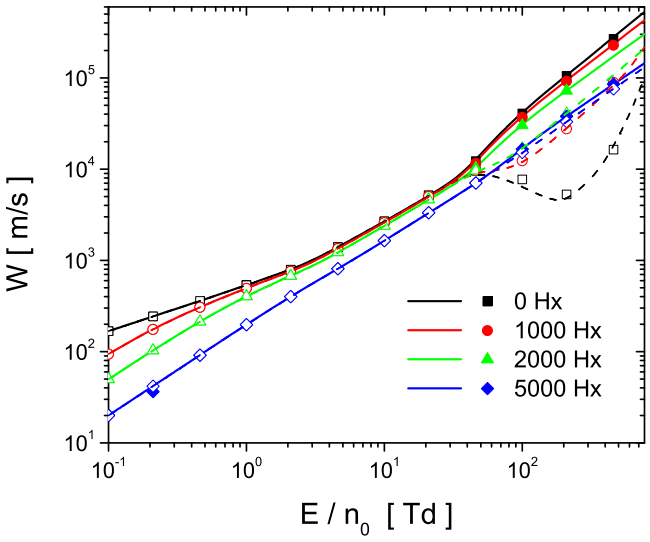

Figure 8. Variation of the flux and bulk drift speed components with E/n_0 for various B/n_0 as indicated on the graph. The results obtained by a Monte Carlo technique are given by symbols (flux values: full symbols; bulk values: open symbols), whereas those obtained by a Boltzmann analysis are presented with lines (flux values: solid lines; bulk values: dashed lines).

magnetic field is applied the bulk drift speed is increased compared to the magnetic field free case for E/n_0 between 40 and 1000 Td, even though for all B/n_0, the effect of Ps formation on drift speed is clearly evident from the existence of differences between the flux and bulk components.

So, physically, why does the NDC phenomenon disappear from the profiles of the drift speed in the presence of magnetic field? How is it that the bulk drift speed is increased

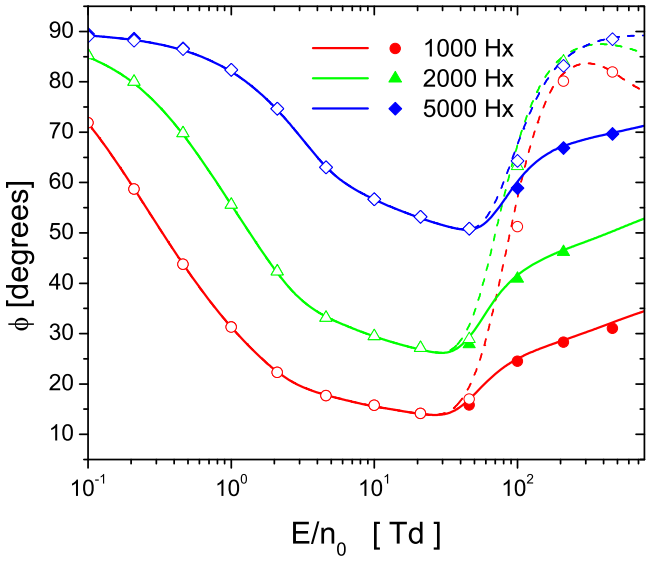

Figure 9. Variation of the magnetic deflection angle with E/n_0 for various B/n_0 as indicated on the graph.

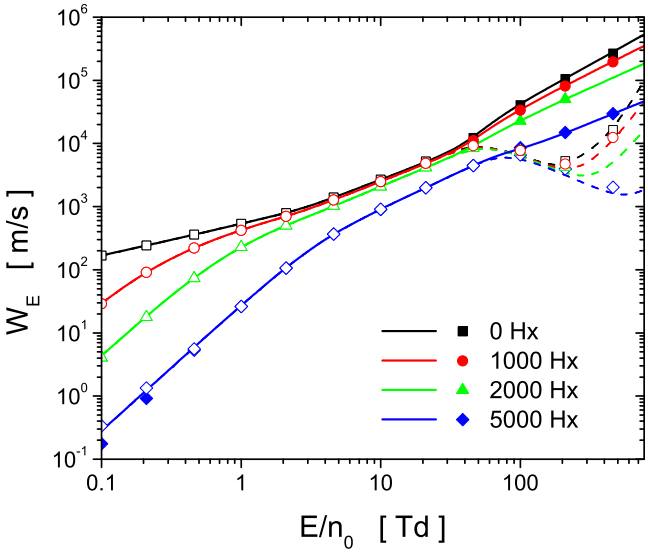

Figure 10. Variation of the longitudinal drift velocity component with E/n_0 for various B/n_0 as indicated on the graph (flux values: full symbols; bulk values: open symbols).

although the positron mean energy is reduced? To address these questions we must consider the longitudinal (**E**) and transverse (**E** × **B**) components of the drift velocity separately, as they exhibit entirely different behaviour in the presence of a magnetic field. The variations of the longitudinal and transverse components with E/n_0 for various B/n_0 are shown in figures 10 and 11, respectively. The profiles of the longitudinal component have a similar shape to those obtained for the magnetic field-free case (see figure 2), although they are lowered and shifted to the right, i.e. towards higher E/n_0. As expected, for a fixed value of E/n_0 the difference

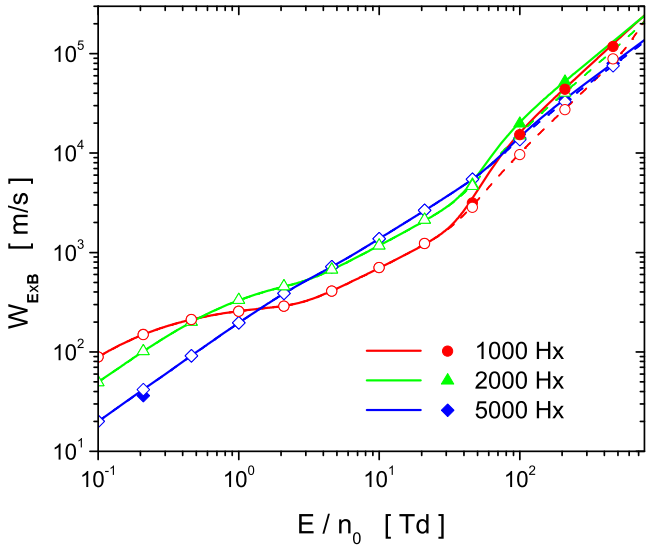

Figure 11. Variation of the transverse drift velocity component with E/n_0 for various B/n_0 as indicated on the graph (flux values: full symbols; bulk values: open symbols).

between the flux and bulk components of $W_{\mathbf{E}}$ is decreased for increasing B/n_0. However, more interesting behaviour is present in the transverse drift velocity component (see figure 11). For all B/n_0 and higher E/n_0 there is a clear difference between the flux and bulk components. A reduction in this difference for increasing B/n_0 is clearly evident. This suggests significant spatial variation in the average energy along the $\mathbf{E} \times \mathbf{B}$ direction, a phenomenon that has never been observed for electrons either in recent Monte Carlo studies of electron transport in electric and magnetic fields [37, 38, 55] or in studies where the transport has been examined by means of a momentum transfer theory [56] and multi-term theory for solving the Boltzmann equation [21, 43, 51]. A clear distinction between the flux and bulk components of $W_{\mathbf{E}\times\mathbf{B}}$ has never been seen for electrons even under conditions where the transport is strongly affected by non-conservative collisions [21]. For positrons in water vapour, due to the combined effects of magnetic field and Ps formation, the bulk component of $W_{\mathbf{E}}$ is actually more affected than the bulk component of $W_{\mathbf{E}\times\mathbf{B}}$, which in turn enhances the contribution of the transverse bulk component in the bulk drift speed. Unlike the bulk components, the flux components behave more 'regularly' and less counterintuitively. Differences between the flux $W_{\mathbf{E}}$ and $W_{\mathbf{E}\times\mathbf{B}}$ components are much less compared to the corresponding differences between the bulk components. This is verified from the profiles of the magnetic deflection angle shown in figure 9. For a B/n_0 of 1000 Hx, we see that the flux magnetic deflection angle stays at about 20°, whereas the bulk value goes to 85° in the energy region where the Ps formation channel is open. This situation is observed only in positron transport, where due to the nature of collisions the flux and bulk drift velocities differ not only in magnitude, but also in direction! Such behaviour may be observed only for positrons in gases where Ps formation is significantly larger than other processes, such as in H_2 [54] and argon [26]. For positrons in N_2 the opposite situation has been reported. The distinction between the flux and bulk components of the magnetic deflection angle in N_2 is significantly diminished. This results from the competition between Ps formation and electronic excitations [30] that are operative in the same energy region.

3.2.2. Tonks' theorem for positrons. The influence of a magnetic field on the electron swarm parameters is often interpreted in terms of the effective reduced electric field concept [52, 55, 57]. In the absence of experimental data, it has not yet been established whether this concept is valid for positrons. In this section, we explore the possibility of using Tonks' theorem (which falls into the category of effective reduced electric field approximations) for positrons with particular emphasis on the existence of NDC in electric and magnetic fields. According to Tonks' theorem [58, 59] and following the previous works for electrons [52, 55, 57], the average positron energy and drift speed are, respectively, given by

$$\begin{aligned} \epsilon(E, B, \Psi) &= \epsilon(E_{\text{eff}}, 0, 0), \\ \mathbf{W}(E, B, \Psi) &= \mathbf{W}(E_{\text{eff}}, 0, 0), \end{aligned} \tag{15}$$

where the combined effect of the electric field, magnetic field and angle between the fields is accounted for by an effective electric field, E_{eff}, whose magnitude is given by [52, 55]

$$E_{\text{eff}}(\epsilon) = E\sqrt{\frac{1 + (\Omega/\nu_m)^2 \cos^2 \Psi}{1 + (\Omega/\nu_m)^2}}. \tag{16}$$

Here Ω is the cyclotron frequency, ν_{m} is the average momentum transfer collision frequency and Ψ is the angle between the fields. Equations (15) and (16) represent a system of nonlinear equations that has been solved iteratively. So using the average momentum transfer collision frequency for the magnetic field-free case, one may attempt to derive the positron transport properties when both the electric and magnetic fields are present.

In figure 12, we show a comparison between the bulk drift speeds for positrons in water vapour obtained by Tonks' theorem and the accurate Monte Carlo method (and/or multi-term approach for solving Boltzmann's equation). Calculations are performed for a range of magnetic field strengths in a crossed field configuration. A very pronounced NDC in the profiles of the bulk drift speed calculated by Tonks' theorem is clearly evident. On the other hand, from accurate data we see that NDC is absent when the magnetic field is applied. Surprisingly, for the mean energy and flux component of the drift speed the agreement is much better (not shown here), particularly in the collision-dominated regime. This is a clear sign that one should be careful in the application of Tonks' theorem for positrons. If Ps formation is a dominant process compared to other inelastic channels, then Tonks' theorem has a restricted domain of validity on the flux drift velocity only. This follows from the fact that Tonks' theorem cannot handle the explicit contribution of Ps formation to the distribution function and the corresponding explicit effects on the drift.

3.2.3. Diffusion of positrons in $\mathbf{E} \times \mathbf{B}$ *fields.* In this section, the synergistic effects of a magnetic field and Ps formation on the diagonal elements of the diffusion tensor are investigated. Before embarking on a discussion, one must be aware that it is hard to fully understand the behaviour of diffusion coefficients in electric and magnetic fields since many parallel factors affect them simultaneously. In addition to the effects of thermal anisotropy (dispersion of positrons due to thermal motion is not the same in different directions) and electric anisotropy (spatial variation of the average energy in conjunction with energy-dependent collision frequency produces differences in the average local velocities for a given direction, which act to inhibit and/or enhance diffusion in that direction), there is the contribution of magnetic anisotropy (due to the explicit orbital effects, the magnetic field always acts to inhibit

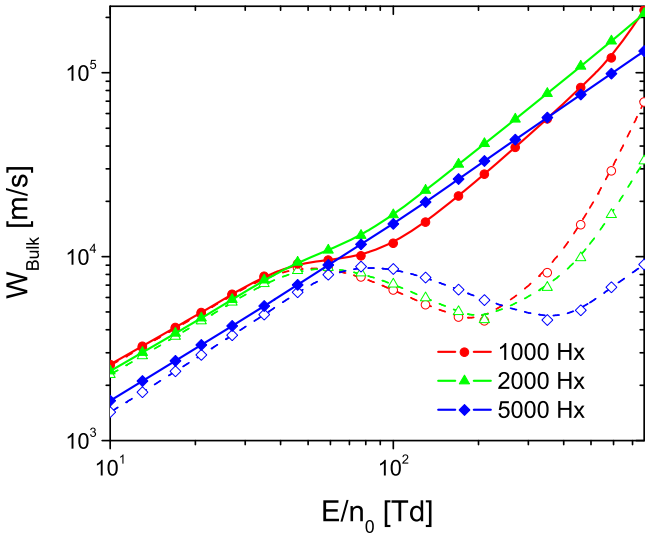

Figure 12. Variation of the bulk components of the drift speed with E/n_0 for various B/n_0 in a crossed field configuration (exact values obtained by a Monte Carlo simulation and/or multi-term approach for solving Boltzmann's equation: solid lines; Tonks' theorem: dashed lines).

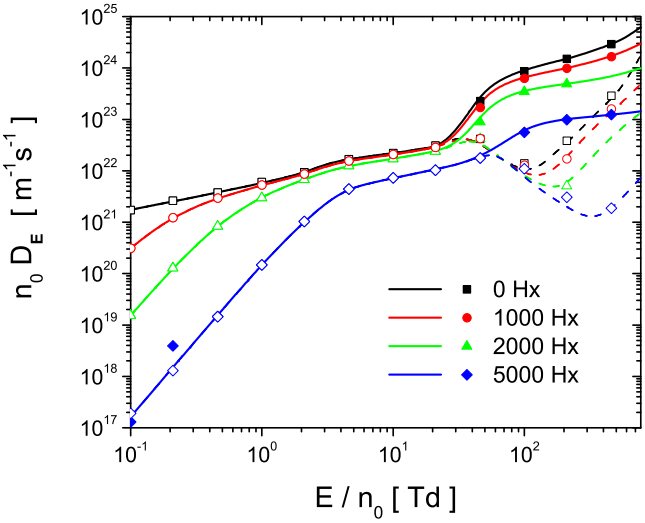

Figure 13. Variation of the bulk and flux components of the longitudinal diffusion coefficient with E/n_0 for various B/n_0 as indicated on the graph.

diffusion in a plane perpendicular to its direction) [21, 24, 44, 51]. In addition, collisions and the complex energy dependence of non-conservative collisions further complicate the issue.

Different diagonal elements of the diffusion tensor show different sensitivities with respect to magnetic field, Ps formation and generally to the energy dependence of the cross-sections. We observe that the longitudinal diffusion coefficient (see figure 13) and transverse diffusion coefficient along the $\mathbf{E} \times \mathbf{B}$ direction (see figure 14) can vary up to five orders of magnitude in the limit of low values of E/n_0 where the behaviour of the swarm is controlled by the

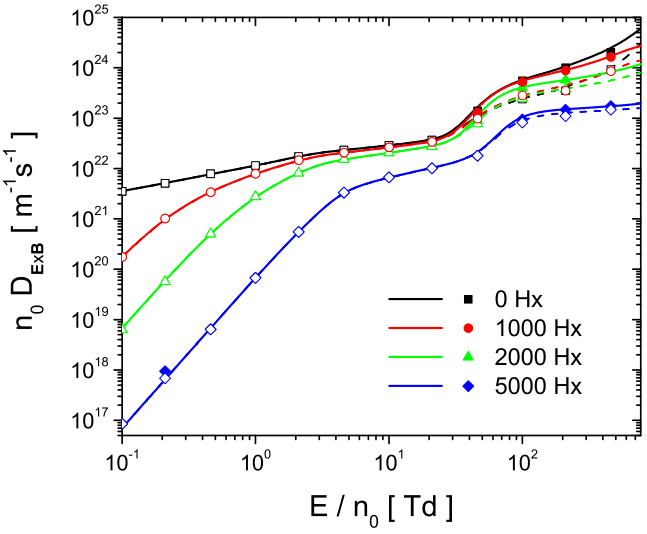

Figure 14. Variation of the bulk and flux components of the transverse diffusion coefficient along the $\mathbf{E} \times \mathbf{B}$ direction with E/n_0 for various B/n_0 as indicated on the graph.

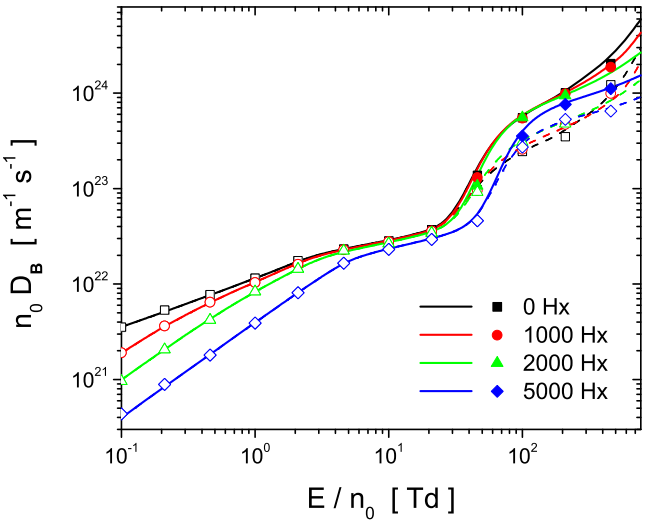

Figure 15. Variation of the bulk and flux components of the transverse diffusion coefficient along the $\mathbf{B}$ direction with E/n_0 for various B/n_0 as indicated on the graph.

magnetic field. The longitudinal diffusion coefficient shows the highest sensitivity with respect to the presence of Ps formation, i.e. differences between the flux and bulk components are much higher for this diffusion coefficient than those observed for the transverse diffusion coefficients along the $\mathbf{E} \times \mathbf{B}$ and $\mathbf{B}$ (see figure 15) directions. In particular, the $n_0 D_{\mathbf{B}}$ component shows the weakest sensitivity to changes of magnetic field. Essentially, it follows the variation of the mean energy with both E/n_0 and B/n_0, and hence the thermal effects play the most important role in the behaviour of this transport property. In conclusion, a better understanding of the synergistic effects of the magnetic field and non-conservative collisions on the diffusion in electric and

magnetic fields requires knowledge of the spatially resolved data along the swarm, particularly those associated with the second-order variations of the average energy. This is beyond the scope of this paper and we defer the detailed discussion on the explicit influence of Ps formation on diffusion processes for positrons in electric and magnetic fields to a future paper.

4. Conclusion

A comprehensive investigation of collision and transport data for positrons in water vapour has been conducted. We have compiled a set of cross-sections for positron scattering in water vapour, which we have used as the input into a combined Monte Carlo simulation and Boltzmann equation analysis of transport properties of positrons and electrons in electric and magnetic fields. There are two motivating factors behind the current programme of investigation. Firstly, there is hope that a swarm analysis like the one performed in this paper is going to trigger a new wave of positron swarm experiments, which would almost certainly improve the normalization and completeness testing of the cross-sections, as well as providing accurate experimental transport data. Secondly, the demand for positron collision and transport data for a wide range of applications has increased considerably. In order to meet this demand and at the same time due to the absence of experimental data, almost certainly in the short term theoretically calculated transport data for positrons will be incorporated into models of various positron-based technologies.

A caution has been issued in this paper on how to deal with the duality of the transport coefficients and how to handle the synergistic effects of magnetic field and Ps formation on the positron transport properties. For the magnetic field-free case, the bulk drift velocity of positrons exhibits a strong NDC effect and physical arguments have been used to explain the nature of this phenomenon. The behaviour of the longitudinal diffusion is also quite striking since differences between the bulk and flux components are more than two orders of magnitude, a phenomenon that has never been reported for electrons. The common practice among positron modellers in the biomedical community of using cross-sections of electrons to describe positron behaviour is clearly problematic, and associated errors have been highlighted here. When a magnetic field is applied, a new level of complexity is introduced. It is shown that the longitudinal and transverse drift velocity components behave in entirely different manners. The bulk component of the longitudinal drift velocity is more affected than the corresponding transverse component, which unexpectedly removes NDC from the profiles of the drift speed.

As detailed in the introduction, this work also serves as a benchmark for any models or simulations of charged particle tracks or the equivalent. Additional tests under non-hydrodynamic conditions would also be a very welcome step in the right direction including investigations of the impact of Ps formation on spatial relaxation behaviour and non-local positron kinetics under steady-state Townsend conditions, in a Frank–Hertz-type experiment or even in a Penning–Malmberg–Surko trap [60]. One can easily adapt the basic phenomenology of positron transport based on a rigorous kinetic theory to a more realistic situation required for modelling PET or radiation therapy. Many of the methods and techniques reported in this paper will carry over to this problem.

As mentioned in the introduction, swarm experiments are desirable for two reasons. They provide a critical test of completeness of the cross-sections and also by adjusting the fields one may vary the mean energy and scan a wide range of cross-sections. In the early studies, however, the initial experiments [12, 13, 61] could not be explained properly, and this may

have contributed to their early disappearance. Nowadays it is evident that an appropriate understanding of the phenomenology and the codes exists which may take into account the dramatically pronounced non-conservative effects and provide the basic data from the transport coefficients affected by Ps formation. The tests involving averaged properties are also a direct verification of the simulation of tracks that is often performed in radiation diagnostics and therapy. The codes able to predict benchmark transport coefficients very accurately are also tested to produce a proper representation of trajectories. The addition of a magnetic field provides a new method to control transport and also to vary the mean energy. Unlike electric fields, the magnetic field may be applied to living organisms.

Tests in a gas are important for the modelling of living organisms as well as for energies beyond a few eV, as the scattering in a liquid is not very different from the scattering in a gas [25]. Finally, the non-conservative Ps formation with its huge cross-section affects transport very much and may provide a really difficult test case for the development of non-conservative transport theories.

Acknowledgments

This work was supported by MNRS Projects ON171037 and III41011 and the Australian Research Council. SD acknowledges support from STW-project 10118, part of the Netherlands Organization for Scientific Research (NWO). The authors are grateful to James Sullivan and Casten Makochekanwa for discussions, ideas and collaboration on some of the topics presented here.

References

[1] Charlton M and Humberston J 2000 *Positron Physics* (New York: Cambridge University Press)
[2] Guessoum N, Ramaty R and Lingenfelter R E 1991 *Astrophys. J.* **378** 170
[3] Hulett L D Jr, Donohue D L, Xu J, Lewis T A, McLuckey S A and Glish G L 1993 *Chem. Phys. Lett.* **216** 236
[4] Muehllehner G and Karp J S 2006 *Phys. Med. Biol.* **51** R117
[5] Surko C M, Passner A, Leventhal M and Wysoki F J 1988 *Phys. Rev. Lett.* **61** 1831
[6] Murphy T J and Surko C M 1992 *Phys. Rev.* A **46** 5696
[7] Sullivan J P, Gilbert S J, Marler J P, Greaves R G, Buckman S J and Surko C M 2002 *Phys. Rev.* A **66** 042708
[8] Marler J P, Sullivan J P and Surko C M 2005 *Phys. Rev.* A **71** 022701
[9] Sullivan J P, Makochekanwa C, Jones A, Caradonna P and Buckman S J 2008 *J. Phys. B: At. Mol. Opt. Phys.* **41** 081001
[10] Makochekanwa C *et al* 2009 *New J. Phys.* **11** 103036
[11] Robson R E 2006 *Introductory Transport Theory for Charged Particles in Gases* (Singapore: World Scientific)
[12] Charlton M 2009 *J. Phys.: Conf. Ser.* **162** 012003
[13] Petrović Lj Z, Banković A, Dujko S, Marjanović S, Šuvakov M, Malović G, Marler J P, Buckman S J, White R D and Robson R E 2010 *J. Phys.: Conf. Ser.* **199** 012016
[14] Kawrakow I 2000 *Med. Phys.* **27** 485
[15] Brown F B (ed) 2003 *MCNP—A General Monte Carlo N-Particle Transport Code, Version 5, Report LA-UR-03-1987* (Los Alamos, NM: Los Alamos National Laboratory)
[16] Agostinelli S S *et al* 2003 *Nucl. Instrum. Methods* A **506** 250–303
[17] Baró J, Sempau J, Fernndez-Varea J M and Salvat F 1995 *Nucl. Instrum. Methods* B **100** 31
[18] Zaidi H 1999 *Med. Phys.* **26** 574
[19] Garcia G, Petrović Lj Z, White R D and Buckman S J 2011 *IEEE Trans. Plasma Sci.* **39** 2962

[20] Champion C and Le Loirec C 2006 *Phys. Med. Biol.* **51** 1707
[21] Dujko S, Petrović Lj Z and Robson R E 2010 *Phys. Rev.* E **81** 046403
[22] Raspopović Z R, Sakadzić S, Bzenić S and Petrović Lj Z 1999 *IEEE Trans. Plasma Sci.* **27** 1241
[23] White R D, Brennan M J and Ness K F 1997 *J. Phys. D: Appl. Phys.* **30** 810
[24] Ness K F 1994 *J. Phys. D: Appl. Phys.* **27** 1848
[25] White R D and Robson R E 2009 *Phys. Rev. Lett.* **102** 230602
[26] Marler J P, Petrović Lj Z, Banković A, Dujko S, Šuvakov M, Malović G and Buckman S J 2009 *Phys. Plasmas* **16** 057101
[27] Šuvakov M, Petrović Lj Z, Marler J P, Buckman S J, Robson R E and Malović G 2008 *New J. Phys.* **10** 053034
[28] Banković A, Petrović Lj Z, Robson R E, Marler J P, Dujko S and Malović G 2009 *Nucl. Instrum. Methods* B **267** 350
[29] Banković A, Dujko S, White R D, Buckman S J and Petrović Lj Z 2011 *Nucl. Instrum. Methods* B at press (doi:10.1016/j.nimb.2011.10.060)
[30] Banković A, Marler J P, Šuvakov M, Malović G and Petrović Lj Z 2008 *Nucl. Instrum. Methods* B **266** 462
[31] White R D, Dujko S, Robson R E, Petrović Lj Z and McEachran R P 2010 *Plasma Sources Sci. Technol.* **19** 034001
[32] White R D, Sullivan J, Bankovic A, Dujko S, Robson R, Petrović Lj Z, García G, Brunger M and Buckman S J 2012 Chapter14: Positron and electron interactions and transport in biological media: modeling tracks and radiation damage *Radiation Damage in Biomolecular Systems, Biological and Medical Physics, Biomedical Engineering* ed G García and M C Fuss (Berlin: Springer Science+Business Media BV)
[33] White R D, Ness K F and Robson R E 2002 *Appl. Surf. Sci.* **192** 26
[34] Kumar K, Skullerud H R and Robson R E 1980 *Aust. J. Phys.* **33** 343
[35] Robson R E, White R D and Petrović Lj Z 2005 *Rev. Mod. Phys.* **77** 1303
[36] Petrovć Lj Z, Raspopović Z M, Dujko S and Makabe T 2002 *Appl. Surf. Sci.* **192** 1
[37] Dujko S, Raspopović Z M and Petrović Lj Z 2005 *J. Phys. D: Appl. Phys.* **38** 2952
[38] Dujko S, White R D, Ness K F, Petrović Lj Z and Robson R E 2006 *J. Phys. D: Appl. Phys.* **39** 4788
[39] Boltzmann L 1872 *Wein. Ber.* **66** 275
[40] Wang-Chang C S, Uhlenbeck G E and DeBoer J 1964 *Studies in Statistical Mechanics* vol 2 ed J DeBoer and G E Uhlenbeck (New York: Wiley) p 241
[41] Ness K F and Robson R E 1986 *Phys. Rev.* A **34** 2185
[42] Robson R E and Ness K F 1986 *Phys. Rev.* A **33** 2086
[43] White R D, Robson R E, Dujko S, Nicoletopoulos P and Li B 2009 *J. Phys. D: Appl. Phys.* **42** 194001
[44] Dujko S 2009 *PhD Thesis* James Cook University, Townsville, Australia
[45] Hayashi M, Pitchford L C, McKoy B V, Chutjian A and Trajmar S (ed) 1987 *Swarm Studies and Inelastic Electron–Molecule Collisions* (New York: Springer)
[46] Petrović Lj Z, Crompton R W and Haddad G N 1984 *Aust. J. Phys.* **37** 23
[47] Petrović Lj Z 1985 *PhD Thesis* Australian National University, Canberra, Australia
[48] Robson R E 1984 *Aust. J. Phys.* **37** 35
[49] Vrhovac S B and Petrović Lj Z 1996 *Phys. Rev.* E **53** 4012
[50] Ness K F and Nolan A M 2000 *Aust. J. Phys.* **53** 437
[51] White R D, Ness K F, Robson R E and Li B 1999 *Phys. Rev.* E **60** 2231
[52] White R D, Robson R E and Ness K F 1999 *IEEE Trans. Plasma Sci.* **27** 1249
[53] White R D, Robson R E, Ness K F and Makabe T 2005 *J. Phys. D: Appl. Phys.* **38** 997
[54] Banković A, Dujko S, White R D, Malović G, Buckman S J and Petrović Lj Z 2011 *J. Phys.: Conf. Ser.* **262** 012007
[55] Petrović Lj Z, Dujko S, Marć D, Malović G, Nikitović Ž, Šašić O, Jovanović J, Stojanović V and Radmilović-Radjenović M 2009 *J. Phys. D: Appl. Phys.* **42** 194002
[56] Li B, Robson R E and White R D 2006 *Phys. Rev.* E **74** 026405

[57] Heylen A E D 1980 *IEE Proc.* **127** 221
[58] Tonks L 1937 *Phys. Rev.* **51** 744
[59] Tonks L and Allis W P 1937 *Phys. Rev.* **52** 710
[60] Marjanović S, Šuvakov M, Banković A, Savić M, Malović G, Buckman S J and Petrović Lj Z 2011 *IEEE Trans. Plasma Sci.* **39** 2614
[61] Bose N, Paul D A L and Tsai J-S 1981 *J. Phys. B: At. Mol. Phys.* **14** L227